

Tributes to pioneers in bioenergetics

BEC Series Editors:

Angelo Azzi, Erich Gnaiger

Cite

Capitanio G, Capitanio N, Papa S (2025) The allosteric protein interactions in the proton pumps of mammalian Complex IV and Complex I of the respiratory chain. *Bioenerg Commun* 2025.1. <https://doi.org/10.26124/bec.2025-0001>

Author contributions

Data curation; Formal analysis; Writing-original draft: GC, NC and SP. Conceptualization: SP.

Conflicts of interest

The authors declare no conflict of interest.

Received 2024-11-24

Reviewed 2024-12-04

Revised 2024-12-12

Accepted 2024-12-31

Published 2025-01-23

Academic editor

Angelo Azzi

Reviewers

Nicoleta Moiso

Marco Colombini

Keywords

Respiratory chain;
Redox proton pump;
Protein allostery;
Cytochrome *c* oxidase;
NADH-ubiquinone
oxidoreductase

The allosteric protein interactions in the proton pumps of mammalian Complex IV and Complex I of the respiratory chain

Giuseppe Capitanio^{1*}, Nazzareno Capitanio², Sergio Papa^{1,‡}

¹ Department of Translational Biomedicine and Neuroscience “DiBrain”, University of Bari “Aldo Moro”, 70124 Bari, Italy.

² Department of Clinical and Experimental Medicine, University of Foggia, Foggia, Italy

‡ Deceased

* Corresponding author: giuseppe.capitanio@uniba.it

Summary

In Complex IV (CIV) of the mammalian respiratory chain, protons are translocated from the matrix (N space) to the Mg²⁺-proton loading site by the combined conformational movements of the subunit I helix X and heme *a* hydroxyfarnesyl. These protons are then released into the intermembrane space (P space) through proton stereochemical transitions in the Cu_A and heme *a* environments.

In Complex I (CI) of mammals, the reduction of benzoquinone bound in the reaction chamber generates a negative wave that drives proton pumping from the N space to the P space via membrane domain translocator(s). During the NADH-ubiquinone oxidoreduction process, four protons are pumped. This can occur either by each of the four membrane domain translocators moving one proton each or by all four protons being pumped by a single translocator, ND5, due to its highly hydrated structure.

This paper aims to elucidate the mechanistic details and structural basis of proton pumping in these complexes, highlighting the role of allosteric protein interactions and the coupling between redox chemistry and proton translocation.

1. Introduction

Allosteric protein interactions are involved in the proton-motive function of respiratory chain [1]. The determining role of allosteric protein interactions in mammalian respiratory complexes NADH-ubiquinone oxidoreductase (CI), ubiquinone cytochrome *c* oxidoreductase (CIII) and cytochrome *c* oxidase (CIV) have been described by Capitanio G., Papa F. and Papa S. [2].

In CIV conformational changes of subunit I, caused by O₂ binding to heme a_3^{2+} -Cu_B⁺ and reduction, and stereochemical transitions coupled to oxidation/reduction of heme *a* and Cu_A, combined with electrostatic effects, determine the proton pumping activity.

In CIII conformational movement of Fe-S protein between cytochromes *b* and *c*₁ is a key element of the proton-motive activity.

In CI ubiquinone binding and reduction result in conformational changes of subunits in the quinone reaction structure which initiate proton pumping.

This study provides new insights into the role of the Mg²⁺-loading site in cytochrome *c* oxidase and explores the mechanism by which quinone redox chemistry in the reaction chamber of NADH-ubiquinone oxidoreductase facilitates proton pumping through the membrane domain translocator(s), thereby advancing our understanding of the fundamental processes underlying mammalian redox-linked proton pumps.

2. Cytochrome *c* oxidase (CIV)

Synchrotron, X-ray crystallography and serial femtosecond X-ray crystallography show that the unwinding of the subunit I helix X is due to binding of O₂ at the reduced binuclear heme a_3 /Cu_B center (BNC) alongside formation of a peroxide intermediate, whilst the rotation of the heme *a* farnesyl OH and the conformational change of subunit I loop I-II are due to heme *a*/Cu_A oxidation (for a detailed discussion about this topic see ref. [2]).

Fully oxidized and fully reduced crystals of bovine CIV identify at the P side a Mg²⁺-proton loading site (PLS), contributed by subunits I and II [3] (Fig.1).

Mg²⁺ is coordinated with the carboxylic group of E198-II, whose carbonyl is coordinated with one copper of the binuclear center. Mg²⁺ is also coordinated with subunit I residues and water molecules, further connected by a hydrogen bond network to heme *a* propionate(s) [3]. In the reduced crystals the coordination angle between Mg²⁺ and E198-II carbonyl increases, breaking a hydrogen bond between H₂O bonded to R439-I and E198-II. This decreases proton translocation capacity between R439-I and E198-II (see [3]). These findings provide a structural basis for the H⁺/e⁻ coupling shared by heme *a* and Cu_A, as revealed by the pH dependence of their redox potentials [4,5].

Detailed studies of proton translocation in liposome-inserted purified bovine-heart CIV (COV) showed the vectorial nature of this H⁺/e⁻ coupling. In these experiments, CIV heme *a* and Cu_A were reduced by succinate using a trace of added frozen-thawed bovine-heart mitochondrial (BHM) and soluble cytochrome *c* or by the photo-activated riboflavin system. Anaerobic oxidation of heme *a* and Cu_A by a stoichiometric amount of ferricyanide, in carbon-monoxide ligated CIV (thus in the absence of the oxygen reduction chemistry), or in the unligated CIV, resulted in the release of 1H⁺ per heme *a* and Cu_A

oxidized in the external space. This proton was taken up upon re-reduction of heme *a* and Cu_A only in the presence of the protonophore CCCP, thus from the internal space of COV [6,7].

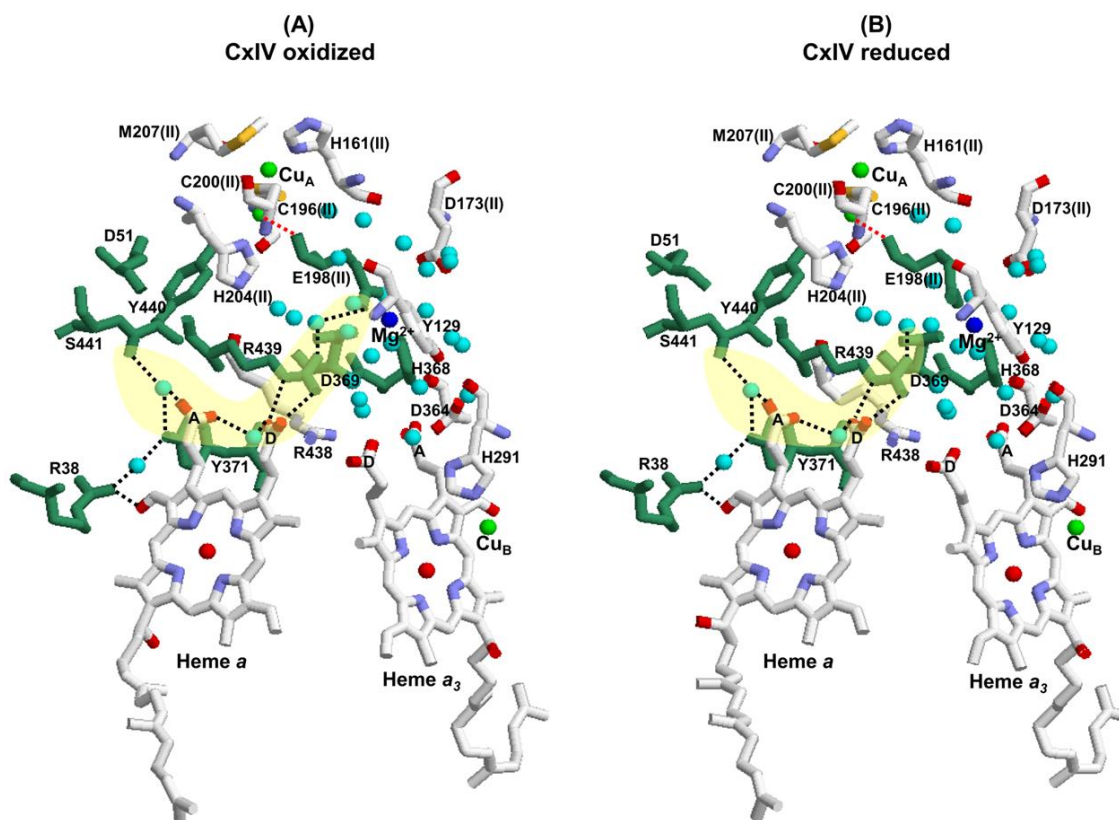


Figure 1. The bovine CIV area above hemes *a* and *a*₃ at the P side in oxidized (A) and reduced (B) X-ray crystals. Structures elaborated using the RasTop 2.2 program and the PDB ID 5B1A and 5B1B for oxidized and reduced CIV respectively. Residues, hemes *a* and *a*₃ are shown as colored sticks. The letters A and D indicate the hemes propionates. Copper, magnesium and iron are shown as green, blue and red balls, respectively. Small light blue balls are H₂O molecules. Hydrogen bonds are drawn as black dotted lines. The amino acid residue E198-II, one of the ligands of Mg²⁺, is also coordinated to Cu_A by the peptide carbonyl (red dotted lines). The residues in green involved together with H₂O in a hydrogen bond network connecting E198-II/Mg²⁺/H₂O cluster with R439-I to the propionate(s) of heme *a* porphyrin are shown in a pale yellow area.

In the CO-ligated CIV COV experiments, the fast release of 1H⁺/CIV oxidized into the external space was a step involving heme *a* and Cu_A in the proton pump (see also [8]). This step was clearly distinct from the slow release of 1H⁺/ferricyanide added, detected upon re-reduction by succinate of the electron carriers (heme *a*, Cu_A and cyt *c*). This slow release was due to scalar H⁺ release in the oxidation of succinate to fumarate in the BHM mediated by redox cycling of added cytochrome *c* in the external space [7]. This invalidates the explanation of the COV experiments presented in a review of the topic [9] that considered the proton translocation simply due to H⁺ release in the oxidation of succinate in the external medium.

Rousseau et al. [10] identified an intermediate (P_R intermediate) of the catalytic cycle by room temperature time resolved optical absorbance changes and femtosecond

XFEL crystallography, showing a conformational change of the subunit I loop I-II (for further details see [2]).

Due to electrostatic repulsion, oxidation of $\text{Fe}a^{2+}$ to $\text{Fe}a^{3+}$ causes the release of one proton from heme *a* in the P space. Heme *a* oxidation also results in the translocation of one proton from the N space to the Mg^{2+} -loading site due to the rotation of the hydroxyfarnesyl group [10]. Upon re-reduction of $\text{Fe}a^{3+}$ by cytochrome *c*, via Cu_A ($\text{P}_R \rightarrow \text{F}$ step of the catalytic cycle), the proton released into the P space from the heme *a* environment is replaced by one proton from the Mg^{2+} -loading site through a hydrogen bond network connecting the Cu_A and heme *a* areas.

These translocation steps effectively pump one proton from the N space to the P space. In the $\text{F} \rightarrow \text{O}_H$, $\text{O}_H \rightarrow \text{E}$ and $\text{E} \rightarrow \text{R}$ steps of the catalytic cycle, three additional protons, one for each step, will be translocated from the N to the P space following the transfer of each electron from cytochrome c^{2+} to O_2 bound at the BNC (see also [2, 11-14]).

A similar mechanism was recently proposed by Rousseau [15], who suggested a heme *a* redox-gate mechanism for proton pumping. In this model, the reduction of heme *a* causes a flip of the farnesyl sidechain from S382 toward S34, resulting in the uptake of a pumped proton from the N-side. Reoxidation of heme *a* by BNC then induces the farnesyl sidechain to rotate back toward S382, allowing the release of a proton to the proton-loading site (via the heme *a* propionates and the R438/R439 moieties). According to this model, each electron transfer from Cu_A to the BNC via heme *a* is accompanied by pumping of one proton from the N- to the P-side.

3. NADH-ubiquinone oxidoreductase (CI)

Cryo-electron microscopy shows that mammalian CI, similar to yeast [16] and prokaryotes [17], has an overall L-shaped structure with a peripheral arm (PA) protruding into the mitochondrial matrix (N-side) and a membrane-integral domain (MD) [18,19-21].

Mammalian CI is made up of 14 subunits, which constitute the minimal functional core conserved from prokaryotes to humans [17,20,21] and 31 supernumerary subunits [20,22]. Seven of the conserved subunits are assembled in the PA, the other seven in the MD. The supernumerary subunits form a shell around the core subunits, stabilizing the complex [20,21].

The ubiquinone reaction chamber joining the PA and MD consists of 49-kDa and PSST subunits, belonging to the PA and ND4L, ND1, ND3 and ND6 subunits belonging to the MD [23]. The MD features three transmembrane subunits: ND5, ND4 and ND2 [23], which have a structure like that of plasma membranes antiporters [24,25]. Each of these three subunits, arranged parallel to each other in the MD, shows discontinuous half-transmembrane helices, with a N terminal part extending from the surface (N-side) and a C terminal part extending to the P side. These parts are connected in the middle of the membrane by conserved Lys/Glu residues [21,23] (see also [17]).

Different mechanisms for the proton pump of CI have been proposed, involving ubiquinone oxidoreduction and conformational changes of the apoproteins reviewed in [1]. Cryo-electron microscopy provides a deep insight into the mechanism of the pump in mammalian CI. These studies [21,23] show that the complex found in different conformations in various species, can be divided into two classes: a closed class and an

open class (see also [26]). Both classes are present in NADH-ubiquinone oxidoreductase active preparations with a prevalence of the closed conformation.

Kampjut and Sazanov [23] analyzed purified ovine CI by cryo-EM crystallography under different conditions, particularly when incubated with NADH and decylubiquinone and flash-frozen during active turnover proton pumping. The cryo-EM structures in the open and closed states show that the loops of the ND1, ND3, ND6, PSST, and 49-kDa subunits adopt different conformations. In the open state, present in native conditions or induced by NADH binding (reviewed in [1]), the loops in subunits ND3, 39-kDa, ND6, and ND1 open, allowing quinone to enter the quinone chamber. This transition to the closed state involves the closure of the ND1 and 49-kDa subunits into retracted conformations, moving the quinone into a deep site close to the N2-FeS center where it is reduced.

Quinone reduction is proposed to involve protonation of Q^{2-} by sequential transfer of two protons from D160 and H59 of the 49-kDa subunit, which are reprotonated by E34 and E70 of the ND4L subunit (see Fig. 5 of ref. [2]). The negative charge generated before protons are taken up from the N space is proposed to induce the pumping of one proton via a proton translocation pathway in the quinone chamber (E-channel) and three additional protons in the three antiporter subunits of the membrane domain ND2, ND4, and ND5 through a complex sequence of electrostatic interactions affecting the protonation of their lysine and glutamic residues located at the junctions of their respective half-transmembrane helices. This aspect requires further clarification [23,27].

Kampjut and Sazanov [28] now propose that, due to the high hydration pattern of the proton input and output pathways of the ND5 subunit—not present in the ND4 and ND2 subunits—and with the E-channel dry on both sides of the membrane, all four protons could be pumped through ND5 (see also [29-31]).

The role of the ND5 subunit as the primary proton exit pathway is further highlighted in a more recent paper by the same authors [32], which analyzed the cryo-electron microscopy structures of *E. coli* CI. The proposed coupling mechanism in this work is based on a 'domino effect' series of proton transfers along the central axis of the MD and electrostatic interactions starting from conformational changes in the quinone chamber and E-channel.

Kampjut and Sazanov [23] proposed that QH_2 moves from the deep reduction site to a shallow site and exits the Q chamber. A critical aspect of this mechanism is how ubiquinone enters and leaves the Q chamber, which appears as a narrow tunnel approximately 30 Å long in the crystal structures of both the open and closed states [33,34]. It has been suggested that the narrow entrance of the Q chamber, forming a bottleneck, could be an artifact of crystallization packing forces, and that molecular dynamics might open the quinone chamber bottleneck [35].

More recently, Gu et al. [36] analyzed by cryo-EM the CI assembled in the porcine purified supercomplex CI-CIII₂-CIV and proposed an alternative mechanism for the proton pump. Vitrified cryo-EM samples were prepared from the supercomplex incubated in different conditions, including one with NADH and Q_{10} . They identified four Q-binding sites in the Q chamber, including site 1 for Q_{10} reduction and site 2 surrounded by charged residues (see Fig. 2).

All the structures supported a Q_{10} molecule invariably bound in the Q chamber. These authors propose, based on the conformations of the subunits obtained by the cryo-EM analysis (see also [37,38]), a two-quinone model. Q_{10} binds to a reduction site (site 1)

in the Q chamber, with the benzoquinone head positioned approximately 10 Å from the N2-FeS center and hydrogen-bonded to Y141 and H92, which also form a hydrogen bond with D193, close to residues of the E channel (Fig. 2A). Q₁₀ is reduced to Q₁₀²⁻ by the N2-FeS center, and Q₁₀²⁻ is protonated to Q₁₀H₂ by H92 and Y141, with the hydrogen bond of D193 broken without movement. Neither are other residue movements observed at site 1 (Fig. 2B). It should be noted that in the analysis by Gu et al., CI is assembled in the supercomplex CI-CIII₂-CIV, while in the work of Kampjut and Sazanov [23], CI was purified as a single entity. Q₁₀H₂ moves to site 2 in the Q chamber, surrounded by charged residues. Gu et al. propose that at site 2, Q₁₀H₂ is oxidized by a second quinone molecule loosely bound at the matrix surface of the complex, approximately 14 Å away from site 2. The Q₁₀²⁻ of the second quinone is protonated to Q₁₀H₂ by matrix protons. Four protons taken up by the matrix are finally released at the external P side. This process is repeated in the following turnover by the movement of Q₁₀ back from site 2 to site 1. However, it is noted that no data on proton uptake from the matrix are discussed, and the site of binding of the second quinone is not characterized (see, however, [39]). The two major aspects of the two-quinone model by Gu et al. are that protons are pumped by the oxidation of Q₁₀H₂ and not by Q₁₀ reduction [23], and the involvement of a second quinone molecule. It can be mentioned here that it was earlier proposed [40,41] (see also [39]) that an SQ⁻/QH₂ involved in proton pumping delivered electrons to a second quinone molecule bound at the matrix side of the complex.

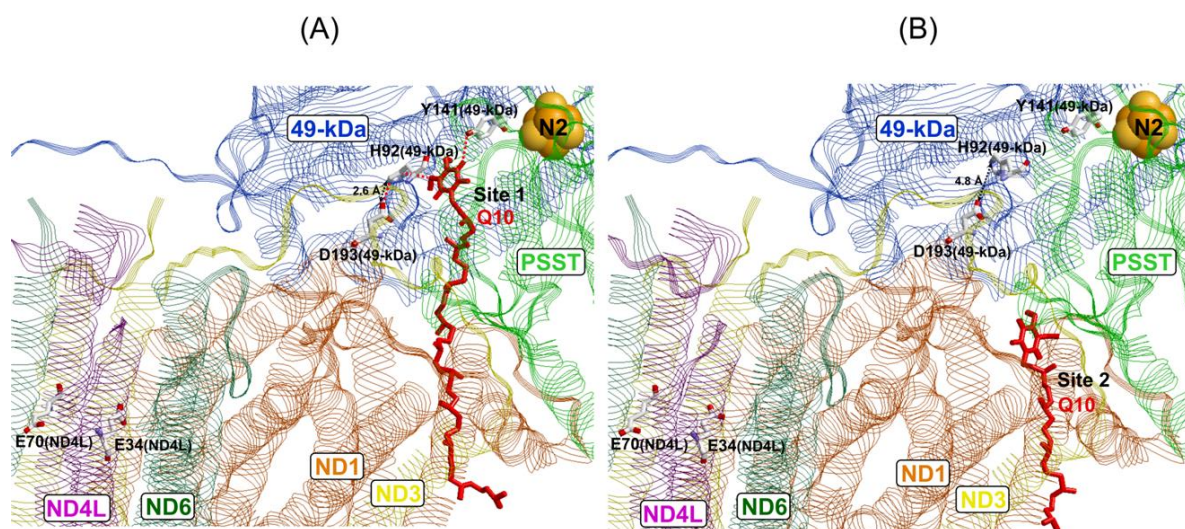


Figure 2. View of the quinone chamber of the porcine CI in a Q₁₀-bound structure (A) and a Q₁₀-NADH-bound structure (B) in active states. The picture was elaborated using the RasTop 2.2 program and the PDB ID 7V2C and 7V2E for (A) and (B) structures respectively. ND4L, ND6, ND1, ND3, PSST and 49-kDa subunits shown in strand mode, N2-FeS center in yellow-orange balls, Q₁₀ molecule and amino acid residues in red and colored sticks respectively. In (A) the Q₁₀ molecule is located at site 1, ≈ 10.2 Å from the N2-FeS center and close to H92 and Y141 of the 49-kDa subunit with which it forms two hydrogen bonds (red dotted lines); H92 also forms another hydrogen bond with D193 of the same subunit (distance between these two residues 2.6 Å, black dotted line). In (B) the Q₁₀ molecule is located at site 2, 24 Å away from the N2-FeS center and due to the movement of H92 the distance between it and D193 increases (4.8 Å) causing the hydrogen bond to break. For further details, see text.

4. Conclusions

In mammalian CIV, protons are translocated from the matrix N side to the Mg^{2+} -proton loading site upon the conformational change in subunit I induced by O_2 binding and reduction at the BNC. The protons at the Mg^{2+} -proton loading site are then expelled into the intermembrane P side by proton stereochemical transitions at the proton loading site. Protons are translocated from the Cu_A environment to the heme *a* environment and then expelled into the P space by the contribution of electrostatic effects.

In mammalian CI, according to Kampjut and Sazanov, reduction of benzoquinone bound in the reaction chamber generates a negative wave that drives proton pumping from the N to the P space by membrane domain translocator(s). Of the four protons pumped in the NADH-ubiquinone oxidoreduction, one proton is translocated by each of the four membrane domain translocators, or instead, all four protons are pumped by one membrane translocator, ND5, due to its highly hydrated structure.

On the other hand, as proposed by Gu et al., this proton pumping is driven by electron transfer from the ubiquinol bound in the reaction pocket to a second quinone-binding site located at the N surface, driving proton pumping from the matrix to the P space. This aspect and the structure of the hypothetical quinone site in the matrix need to be clarified by further inspection.

Acknowledgments Funding

Grants from Ministero dell'Istruzione, dell'Università e della Ricerca (MIUR), Italy and University of Bari "Aldo Moro."

Dedicated to the memory of Alexander A. Konstantinov who made important contribution to the proton pump of CIV.

References

- [1] Papa S, Capitanio G, Papa F (2018) The mechanism of coupling between oxido-reduction and proton translocation in respiratory chain enzymes. <https://doi.org/10.1111/brv.12347>
- [2] Capitanio G, Papa F, Papa S (2021) The allosteric protein interactions in the proton-motive function of mammalian redox enzymes of the respiratory chain. <https://doi.org/10.1016/j.biochi.2021.05.018>
- [3] Yano N, Muramoto K, Shimada A, Takemura S, Baba J, Fujisawa H, Mochizuki I, Shinzawa-Itoh K, Yamashita E, Tsukihara T, et al. (2016) The Mg^{2+} -containing water cluster of mammalian cytochrome *c* oxidase collects four pumping proton equivalents in each catalytic cycle. <https://doi.org/10.1074/jbc.M115.711770>
- [4] Capitanio N, Capitanio G, Minuto M, De Nitto E, Palese LL, Nicholls P, Papa S (2000) Coupling of electron transfer with proton transfer at heme *a* and Cu_A (redox Bohr effects) in cytochrome *c* oxidase. Studies with the carbon monoxide inhibited enzyme. <https://doi.org/10.1021/bi0003137>
- [5] Capitanio N, Capitanio G, Boffoli D, Papa S (2000) The proton/electron coupling ratio at heme *a* and Cu_A in bovine heart cytochrome *c* oxidase. <https://doi.org/10.1021/bi001940z>
- [6] Capitanio N, Capitanio G, De Nitto E, Papa S (1997) Vectorial nature of redox Bohr effects in bovine heart cytochrome *c* oxidase. [https://doi.org/10.1016/s0014-5793\(97\)01043-0](https://doi.org/10.1016/s0014-5793(97)01043-0)

- [7] Capitanio G, Martino PL, Capitanio N, Papa S (2011) Redox Bohr effects and the role of heme *a* in the proton pump of bovine heart cytochrome *c* oxidase. <https://doi.org/10.1016/j.bbabi.2011.02.004>
- [8] Artzatbanov VY, Konstantinov AA, Skulachev VP (1978) Involvement of intramitochondrial protons in redox reactions of cytochrome *a*. [https://doi.org/10.1016/0014-5793\(78\)80327-5](https://doi.org/10.1016/0014-5793(78)80327-5)
- [9] Wikstrom M, Krab K, Sharma V (2018) Oxygen activation and energy conservation by cytochrome *c* oxidase. <https://doi.org/10.1021/acs.chemrev.7b00664>
- [10] Ishigami I, Lewis-Ballester A, Echelmeier A, Brehm G, Zatsopin NA, Grant TD, Coe JD, Lisova S, Nelson G, Zhang S, et al. (2019) Snapshot of an oxygen intermediate in the catalytic reaction of cytochrome *c* oxidase. <https://doi.org/10.1073/pnas.1814526116>
- [11] Shimada A, Kubo M, Baba S, Yamashita K, Hirata K, Ueno G, Nomura T, Kimura T, Shinzawa-Itoh K, Baba J, et al. (2017) A nanosecond time-resolved XFEL analysis of structural changes associated with CO release from cytochrome *c* oxidase. <https://doi.org/10.1126/sciadv.1603042>
- [12] Tsukahara T, Shimokata K, Katayama Y, Shimada H, Muramoto K, Aoyama H, Mochizuki M, Shinzawa-Itoh K, Yamashita E, Yao M, et al. (2003) The low-spin heme of cytochrome *c* oxidase as the driving element of the proton-pumping process. <https://doi.org/10.1073/pnas.2635097100>
- [13] Shimada A, Hara F, Shinzawa-Itoh K, Kanehisa N, Yamashita E, Muramoto K, Tsukahara T, Yoshikawa S (2021) Critical roles of the Cu_B site in efficient proton pumping as revealed by crystal structures of mammalian cytochrome *c* oxidase catalytic intermediates. <https://doi.org/10.1016/j.jbc.2021.100967>
- [14] Capitanio G, Palese LL, Papa F, Papa S (2020) Allosteric cooperativity in proton energy conversion in A1-type cytochrome *c* oxidase. <https://doi.org/10.1016/j.jmb.2019.09.027>
- [15] Rousseau DL, Ishigami I, Yeh SR (2025) Structural and functional mechanisms of cytochrome *c* oxidase. <https://doi.org/10.1016/j.jinorgbio.2024.112730>
- [16] Leonard K, Haiker H, Weiss H (1987) Three-dimensional structure of NADH:ubiquinone reductase (complex I) from *Neurospora* mitochondria determined by electron microscopy of membrane crystals. [https://doi.org/10.1016/0022-2836\(87\)90375-5](https://doi.org/10.1016/0022-2836(87)90375-5)
- [17] Baradaran R, Berrisford JM, Minhas GS, Sazanov LA (2013) Crystal structure of the entire respiratory Complex I. <https://doi.org/10.1038/nature11871>
- [18] Wu M, Gu J, Guo R, Huang Y, Yang M (2016) Structure of mammalian respiratory supercomplexes I₁III₂IV₁. <https://doi.org/10.1016/j.cell.2016.11.012>
- [19] Letts JA, Sazanov LA (2017) Clarifying the supercomplexes: the higher-order organization of the mitochondrial electron transport chain. <https://doi.org/10.1038/nsmb.3460>
- [20] Fiedorczuk K, Letts JA, Degliesposti G, Kaszuba K, Skehel M, Sazanov LA (2016) Atomic structure of the entire mammalian mitochondrial Complex I. <https://doi.org/10.1038/nature19794>
- [21] Agip ANA, Blaza JN, Bridges HR, Viscomi C, Rawson S, Muench SP, Hirst J (2018) Cryo-EM structures of Complex I from mouse heart mitochondria in two biochemically defined states. <https://doi.org/10.1038/s41594-018-0073-1>
- [22] Carroll J, Fearnley IM, Skehel JM, Shannon RJ, Hirst J, Walker JE (2006) Bovine complex I is a complex of 45 different subunits. <https://doi.org/10.1074/jbc.M607135200>
- [23] Kampjut D, Sazanov LA (2020) The coupling mechanism of mammalian respiratory Complex I. <https://doi.org/10.1126/science.abc4209>

- [24] Fearnley IM, Walker JE (1992) Conservation of sequences of subunits of mitochondrial complex I and their relationships with other proteins. [https://doi.org/10.1016/0005-2728\(92\)90001-I](https://doi.org/10.1016/0005-2728(92)90001-I)
- [25] Mathiesen C, Hägerhäll C (2002) Transmembrane topology of the NuoL, M and N subunits of NADH:quinone oxidoreductase and their homologous among membrane-bound hydrogenases and bona fide antiporters. [https://doi.org/10.1016/S0005-2728\(02\)00343-2](https://doi.org/10.1016/S0005-2728(02)00343-2)
- [26] Chung I, Grba DN, Wright JJ, Hirst J (2022) Making the leap from structure to mechanism: are the open states of mammalian Complex I identified by cryoEM resting states or catalytic intermediates? <https://doi.org/10.1016/j.sbi.2022.102447>
- [27] Mühlbauer ME, Saura P, Nuber F, Di Luca A, Friedrich T, Kaila VRI (2020) Water-gated proton transfer dynamics in respiratory complex I. <https://doi.org/10.1021/jacs.0c02789>
- [28] Kampjut D, Sazanov LA (2022) Structure of respiratory complex I – An emerging blueprint for the mechanism. <https://doi.org/10.1016/j.sbi.2022.102350>
- [29] Parey K, Lasham J, Mills DJ, Djurabekova A, Haapanen O, Yoga EG, Xie H, Kühlbrandt W, Sharma V, Vonck J, et al. (2021) High-resolution structure and dynamics of mitochondrial complex I – Insights into the proton pumping mechanism. <http://doi.org/10.1126/sciadv.abj3221>
- [30] Nuber F, Schimpf J, di Rago J-P, Tribouillard-Tanvier D, Procaccio V, Martin-Negrier M-L, Trimouille A, Biner O, von Ballmoos C, Friedrich T (2021) Biochemical consequences of two clinically relevant ND-gene mutations in *Escherichia coli* respiratory complex I. <https://doi.org/10.1038/s41598-021-91631-3>
- [31] Hooser F, Tausend H, Götz S, Wohlwend D, Einsle O, Günther S, Friedrich T (2022) Respiratory complex I with charge symmetry in the membrane arm pumps protons. <https://doi.org/10.1073/pnas.2123090119>
- [32] Kravchuk V, Petrova O, Kampjut D, Wojciechowska-Bason A, Breese Z, Sazanov L (2022) A universal coupling mechanism of respiratory complex I. <https://doi.org/10.1038/s41586-022-05199-7>
- [33] Wang P, Dhananjayan N, Hagraas MA, Stuchebrukhov AA (2021) Respiratory complex I: bottleneck at the entrance of quinone site requires conformational change for its opening. <https://doi.org/10.1016/j.bbabi.2020.148326>
- [34] Galemou Yoga E, Schiller J, Zickermann V (2021) Ubiquinone binding and reduction by complex I – open questions and mechanistic implications. <https://doi.org/10.3389/fchem.2021.672851>
- [35] Dhananjayan N, Wang P, Leontyev I, Stuchebrukhov AA (2022) Quinone binding in respiratory complex I: going through the eye of a needle. The squeeze-in mechanism of passing the narrow entrance of the quinone site. <https://doi.org/10.1007/s43630-021-00113-y>
- [36] Gu J, Liu T, Guo R, Zhang L, Yang M (2022) The coupling mechanism of mammalian mitochondrial complex I. <https://doi.org/10.1038/s41594-022-00722-w>
- [37] Sharma V, Belevich G, Gamiz-Hernandez AP, Rög T, Vattulainen I, Verkhovskaya ML, Wikstrom M, Hummer G, Kaila VRI (2015) Redox-induced activation of the proton pump in the respiratory complex I. <https://doi.org/10.1073/pnas.1503761112>
- [38] Le Breton N, Wright JJ, Jones AJY, Salvadori E, Bridges HR, Hirst J, Roessler MM (2017) Using hyperfine electron paramagnetic resonance spectroscopy to define the proton-coupled electron transfer reaction at Fe-S cluster N2 in respiratory complex I. <https://doi.org/10.1021/jacs.7b09261>

- [39] Djurabekova A, Galemou Yoga E, Nyman A, Pirttikoski A, Zickermann V, Haapanen O, Sharma V (2022) Docking and molecular simulations reveal a quinone-binding site on the surface of respiratory complex I. <https://doi.org/10.1002/1873-3468.14346>
- [40] Papa S, Capitanio N, Villani G (1999) Proton pumps of respiratory chain enzymes. In: Papa S, Guerrieri F, Taeger JM (Eds.), *Frontiers of Cellular Bioenergetics: Molecular Biology, Biochemistry and Physiopathology*. Plenum Press, London and New York, pp. 49-88.
- [41] Ohnishi T, Salerno JC (2005) Conformational-driven and semiquinone-gated proton-pump mechanism in the NADH-ubiquinone oxidoreductase (complex I). <https://doi.org/10.1016/j.febslet.2005.06.086>

Copyright © 2025 The authors. This Open Access peer-reviewed communication is distributed under the terms of the Creative Commons Attribution License, which permits unrestricted use, distribution, and reproduction in any medium, provided the original authors and source are credited. © remains with the authors, who have granted BEC an Open Access publication license in perpetuity.

